Analytical and Bioanalytical Chemistry
https://doi.org/10.1007/s00216-024-05493-5

RESEARCH PAPER

Real-time monitoring of voltage-responsive biomolecular binding onto electro-switchable surfaces

Nathan E. Pringle[1] · Paula M. Mendes[2] · Walter F. Paxton[1]

Received: 3 July 2024 / Revised: 9 August 2024 / Accepted: 12 August 2024

Abstract

Voltage-responsive biosensors capable of monitoring real-time adsorption behavior of biological analytes onto electroactive surfaces offer attractive strategies for disease detection, separations, and other adsorption-dependent analytical techniques. Adsorption of biological analytes onto electrically switchable surfaces can be modelled using neutravidin and biotin. Here, we report self-assembled monolayers formed from voltage-switchable biotinylated molecules on gold surfaces with tunable sensitivity to neutravidin in response to applied voltages. By using electrochemical quartz crystal microbalance (EQCM), we demonstrated real-time switchable behavior of these bio-surfaces and investigate the range of sensitivity by varying the potential of the same surfaces from −400 mV to open circuit potential (+155 mV) to +300 mV. We compared the tunability of the mixed surfaces to bare Au surfaces, voltage inert surfaces, and switchable biotinylated surfaces. Our results indicate that quartz crystal microbalance allows real-time changes in analyte binding behavior, which enabled observing the evolution of neutravidin sensitivity as the applied voltage was shifted. EQCM could in principle be used in kinetic studies or to optimize voltage-switchable surfaces in adsorption-based diagnostics.

Keywords Self-assembled monolayers · Voltage-responsive surfaces · Biosensors · Adsorption · Electrochemistry · Real-time measurements

Introduction

Stimuli-responsive biological surfaces hold great promise for immunoassay and biosensor design for *in situ* and *in vivo* disease detection. These surfaces can modulate biomolecule activity [1–5] and protein adhesion [6, 7] in response to external stimuli at the liquid-solid interface. Understanding these surfaces and how to control them will greatly aid the development of reagent-less, sensitive, reusable, and real-time biosensors [8] with tunable properties. Similar surfaces have been used to capture or release DNA [9], proteins [10], antibodies [11], and cells [12] in response to photo-, electrochemical-, electrical-, or thermal-stimuli. Voltage-switchable surfaces modulate the behavior and properties of a surface in response to applied potentials [2–5, 13–16]. By forming self-assembled monolayers containing charged functional groups, the conformation of the molecules can respond electrostatically to applied potentials [13, 14, 17–19]. The conformation change can hide or present a functionalized head group, enabling dynamic, reversible control of the properties of the liquid-surface interface [13–17].

The properties of voltage-responsive surfaces have been studied using self-assembled monolayers composed of charged oligopeptides with terminal biotin moieties adsorbed to a metallic electrode [13]. The terminal biotin binds neutravidin with one of the strongest noncovalent interactions found in nature (K_a = ~10^{15} M^{-1}) [20], allowing investigation of voltage-tunable sensitivity of the surface to the presence of neutravidin in solution. Mendes et al. demonstrated that the application of a negative or positive potential to the surface significantly inhibited or promoted neutravidin binding respectively by hiding or exposing the terminal neutravidin moiety (Fig. 1) [13]. The mechanism illustrated in Fig. 1 for mixed monolayers of TEGT and Biotin–KKKKC has been previously characterized by XPS [13] and in situ sum-frequency generation to demonstrate the change of conformation of the molecules on both states

✉ Walter F. Paxton
paxton@chem.byu.edu

[1] Department of Chemistry and Biochemistry, Brigham Young University, C100 BNSN, Provo, UT 84602, USA

[2] School of Chemical Engineering, University of Birmingham, Edgbaston, Birmingham B15 2TT, UK

Published online: 22 August 2024

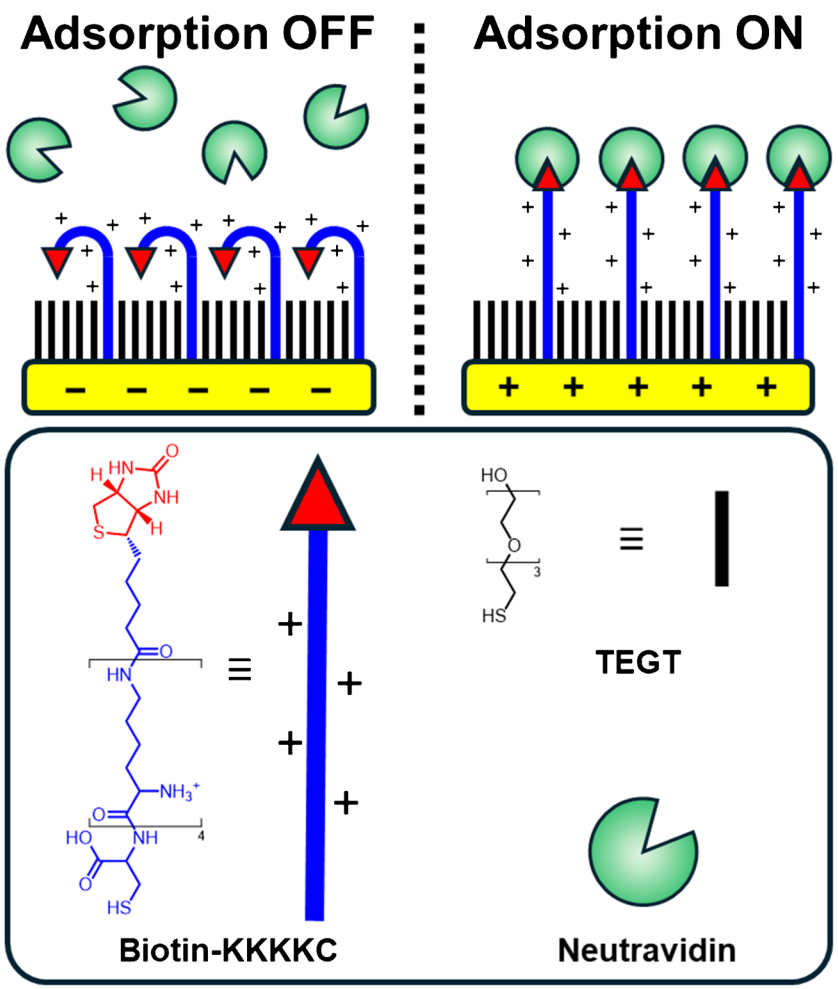

Fig. 1 Schematic representation of the response of biosensor composed of charged "detector" molecules (Biotin–KKKKC) and "spacer" molecules (TEGT) to changes in applied potential. The mechanism of tunability of binding events in response to applied potentials is shown. The structures of Biotin–KKKKC and TEGT are also shown

[16, 17]. These studies include demonstrating control over adsorption of neutravidin at different potentials using electrochemical surface plasmon resonance (eSPR). However, the full range of neutravidin sensitivity of these surfaces by taking a single surface from lowest to highest sensitivity has not been investigated. Studying the full range of the sensor response to voltage enables investigation of time dependence of binding events and the evolution of surface properties as a function of applied potential in real time.

In contrast to ESPR used previously [8, 11], electrochemical quartz crystal microbalance (EQCM) avoids the complications of surface plasmon resonance responses that change with both surface adsorption and applied potential. Using EQCM, we studied the range of neutravidin sensitivity of these surfaces as a function of applied potential. We formed and characterized an inert monolayer (TEGT), a monolayer of a charged moiety with affinity for neutravidin (Biotin–KKKKC), and a mixed monolayer that includes both components. We then observed the neutravidin binding behavior of each surface under the sequential application of different potentials. The mixed Biotin–KKKKC/TEGT surface was substantially more sensitive to the presence of neutravidin at positive potentials, displaying the highest tunability in neutravidin binding compared to the Biotin–KKKKC and TEGT surfaces. Real-time monitoring of these voltage-switchable surfaces will enable future kinetic studies of binding events and the optimization of sensitivity as a function of applied potential.

Experimental

Materials We used sodium phosphate (EMD chemicals); neutravidin (ThermoFisher); Biotin–KKKKC (custom synthesized by and purchased from PeptideSynthetics, UK); 2–{2–[2–(2–mercaptoethoxy)ethoxy]ethoxy}ethanol (TEGT, ThermoFisher); ethanol; triethylamine; and phosphoric acid, as received and without further purification. Deionized water was prepared from a commercial water purification system (Synergy UV–R, Millipore). Sodium phosphate buffer solution (100 mM Na_3PO_4) was adjusted to pH = 7 with concentrated H_3PO_4. Ethanolic solution for SAM formation was prepared from 190 proof ethanol and triethylamine (3% v/v) [13].

Preparation of self-assembled monolayers The self-assembled monolayers were formed using thiol molecules on gold-coated QCM sensors. Monolayer formation was monitored by quartz crystal microbalance (QCM, Nanoscience Instruments, Inc.), using gold-coated silicon crystals (QSX301) with a surface area of 1.0 cm^2 and a mass sensitivity of -17.7 ng Hz^{-1} cm^{-2} in an electrochemical QCM (EQCM) cell. The sensor crystals were cleaned with 2% v/v Hellmanex III; deionized water (rinse); isopropyl alcohol; and deionized water (rinse); and then dried under a stream of nitrogen. Next, the sensors were cleaned by RF plasma treatment under a reduced ambient air pressure using a commercial plasma cleaner (PDC–32G, Harrick Plasma). For measurements, the standard error of the normalized change in resonant frequency is <0.3 Hz for all overtones. Data were analyzed using commercial software (QTools, Nanoscience Instruments, Inc.). Self-assembled monolayers were formed on gold QCM sensors after first equilibrating the sensor in ethanolic solution and then pumping ethanolic solutions of TEGT, Biotin–KKKKC, or 1:40 Biotin–KKKKC/TEGT (0.1 mM total thiol concentration) into the sensor chamber. 1:40 Biotin–KKKKC/TEGT solution has been demonstrated to form SAMs with ~1:16 Biotin–KKKKC/TEGT on the surface [24], which will be referred to as *mixed monolayers* for the remainder of this work. This compositional ratio prevents Biotin–KKKKC molecules from sterically hindering adjacent molecules during potential-induced conformational changes [13, 17]. The thiol solution was incubated on the surface for at least 5 min, or until the Δf of the QCM response was less than 0.5 Hz min^{-1}. Following incubation, the monolayer was rinsed by pumping ethanolic solution into the sensor chamber for at least 5 min, or until the Δf of the QCM response was less than 0.5 Hz min^{-1}. Following characterization by QCM, the ethanolic solution was replaced with 100 mM sodium phosphate buffer solution (PBS) pH = 7 for the electrochemical experiments.

Electrochemical measurements We used an electrochemical QCM (EQCM) cell to monitor the formation of the monolayer and perform electrochemical experiments. All experiments were conducted at pH = 7 and room temperature in phosphate buffer. The EQCM cell was connected to an electrochemical analyzer (CHI600, CH Instruments) serving as a voltmeter and ammeter, with either bare or monolayer-coated gold sensors as the working electrode. The counter electrode consisted of a platinum plate. The reference used for all applied and measured open circuit potentials (OCP) was an Ag/AgCl reference electrode (QSP020, WPI Instruments). For monolayer stability measurements and conformation change investigation, cyclic voltammetry from +300 mV to −400 mV and voltage-STEP measurements at the limiting potentials were performed in 100 mM phosphate buffer (pH = 7) while monitoring changes in frequency and dissipation via EQCM.

Neutravidin binding measurements All neutravidin adsorption experiments were conducted using 10 μg mL^{-1} neutravidin in 100 mM PBS buffer (pH = 7). The neutravidin adsorption was monitored by quartz crystal microbalance at −400 mV, OCP (+155 ± 59 mV), and +300 mV relative to an Ag/AgCl reference electrode. In the tests with the TEGT, mixed monolayers, and bare Au surfaces, we established a stable 5-min baseline in 100 mM PBS buffer, applied −400 mV, then waited for 2 min for the EQCM measurement to stabilize. Once stable, we flowed the neutravidin solution through the cell at a rate of 200 μL min^{-1} for 1 min, then slowed the flow rate to 10 μL min^{-1} for the duration of the experiment. Once Δf was stable at −400 mV, we returned the surface to OCP while continuing to monitor the adsorption of neutravidin. Once the amount of bound neutravidin stabilized, we applied +300 mV to the surface until the mass adsorbed stabilized. We then returned the surface to OCP and rinsed the surface for 5 min with PBS buffer. Due to the large amount of neutravidin adsorbed by the Biotin–KKKKC SAMs, the pump speed of neutravidin solution was kept at 200 μL min^{-1} to ensure complete surface saturation.

Results and discussion

Monolayer formation and characterization To investigate the tunable neutravidin binding behavior of biotinylated SAMs on gold electrodes, we prepared monolayers from solutions of TEGT, Biotin–KKKKC, and 1:40 Biotin–KKKKC/TEGT. The observed changes in the resonant frequency (Δf) from the quartz crystal microbalance (QCM) upon introduction of each solution confirmed the successful adsorption of each monolayer on gold surfaces (Fig. 2). Using Δf, we calculated the mass density of adsorbed molecules using the simplified Sauerbrey equation (Eq. 1) which relates the change in the measured resonant frequency of the nth overtone, Δf_n, to the adsorbed mass, Δm, using the mass sensitivity of the sensor, $C = -17.7$ ng Hz^{-1} cm^{-2} [21].

$$\Delta m = \Delta f_n * \frac{C}{n} \tag{1}$$

We calculated the molecular density of the TEGT and Biotin–KKKKC monolayers by dividing the adsorbed mass by the molecular mass of the adsorbate (Table 1). In our experiments, Δf_n indicates a relative amount of the analyte which can be calibrated to particular concentrations of mass response. Using the Sauerbrey equation allows the measured Δf_n to relate to an absolute, rather than relative, amount of adsorption. Our use of the Sauerbrey relationship to determine the amount of adsorbed mass on the surface in place

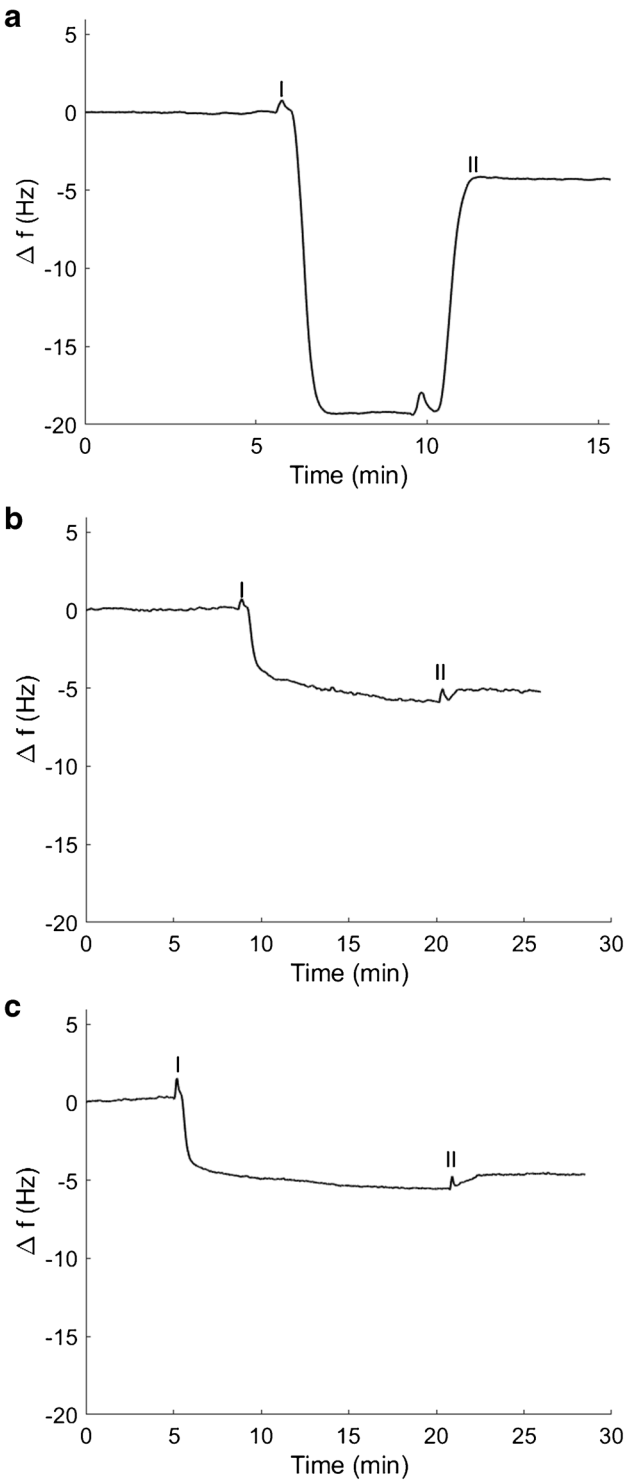

Fig. 2 Representative QCM measurements of Δf (normalized to the third overtone, i.e., $\Delta f = \Delta f_3/3$) for the adsorption of TEGT (**a**), Biotin–KKKKC (**b**), and mixed monolayers (**c**) from 0.1 mM ethanolic solutions at 20 °C. The marks on the graph correspond to the introduction of the monolayer solution (I) and the buffer rinse (II)

of the viscoelastic model is valid because the ratio of $|\Delta D_n/(\Delta f_n/n)| << 4 \times 10^{-7}$ Hz^{-1} for all monolayers following the buffer rinse [22]. The molecular density of the mixed monolayer was unable to be calculated directly from the QCM data due to multiple molecules being bound to the surface.

Electrochemical stability Following the characterization of each monolayer using QCM, we exchanged the ethanolic buffer solution for 100 mM aqueous neutral phosphate buffer solution (PBS) at pH = 7. We assessed the electrochemical stability of each monolayer from −400 mV to +300 mV by performing cyclic voltammetry (CV) (Fig. 3). We did not observe any significant surface reduction or oxidation peaks across this voltage range with any of the surface types, or any indications of monolayer desorption. This potential window contains the double-layer region for each monolayer. Successful adsorption of the monolayer is indicated by a reduction in the double-layer capacitance of the surface (Fig. 3A, B, C) when compared to a bare Au surface (Fig. 3D). These results confirmed surface adsorption and indicated that the surface-adsorbed molecules are stable within this electrochemical window; therefore, the electrochemical window used in our experiments was appropriate for modifying the potential of the surface without causing degradation of the monolayers.

Neutravidin binding behavior of each surface Previously, Mendes et al. demonstrated minimal, intermediate, and maximal neutravidin binding using 1:16 Biotin–KKKKC/TEGT surfaces when applying a constant −400 mV, OCP (+155 mV), or +300 mV using electrochemical surface plasmon resonance (eSPR), an optical technique [13]. A limitation of eSPR is that applying a potential to the surface changes the charge density of the sensor, modulating the dielectric properties of the eSPR surface and changing the response of the surface [23]. As a result, Mendes et al. had to equilibrate the instrument response at the applied potential prior to introducing neutravidin solution [13, 16]. This prevented the real-time study of the full range of neutravidin sensitivity as a function of potential on the same surface [13].

An advantage of the EQCM cell is the ability to apply multiple potentials to the same surface without significantly changing the measured instrumental response. This enabled us to take mixed monolayers through their full range of sensitivity in the presence of neutravidin. To do this, we applied −400 mV and introduced neutravidin solution. Once Δf was stable at −400 mV, we returned the surface to OCP while continuing to monitor the adsorption of neutravidin. Once the amount of bound neutravidin stabilized (i.e., when $\Delta f <$ 0.2 Hz/min), we applied +300 mV to the surface until the mass adsorbed stabilized. We then returned the surface to OCP and rinsed the surface for 5 min with PBS buffer. The

Table 1 Mass coverage and molecular densities from QCM measurements of Biotin–KKKKC, TEGT, and mixed SAMs

SAM type	Molar mass (g mol^{-1})	Δf (Hz)[a]	Adsorbed mass (ng cm^{-2})	Molecular density (molecules cm^{-2})[b]
TEGT	166.17	−3.6 (0.4)	63.7 (7.1)	$2.6 \pm 0.3 \times 10^{14}$
Biotin–KKKKC	880.126	−5.3 (0.6)	93.8 (10.6)	$6.5 \pm 0.8 \times 10^{13}$
1:16 Biotin–KKKKC/TEGT	N/A[c]	−3.5 (0.2)	62.0 (3.54)	N/A[c]

[a]From QCM data for the third overtone; standard error of the mean from at least 3 measurements in parentheses

[b]Molecular density from QCM data calculated using Eq. 1 and the molecular weight of the respective compounds

[c]Unable to be calculated since the Biotin–KKKKC/TEGT ratio cannot be detected directly using QCM

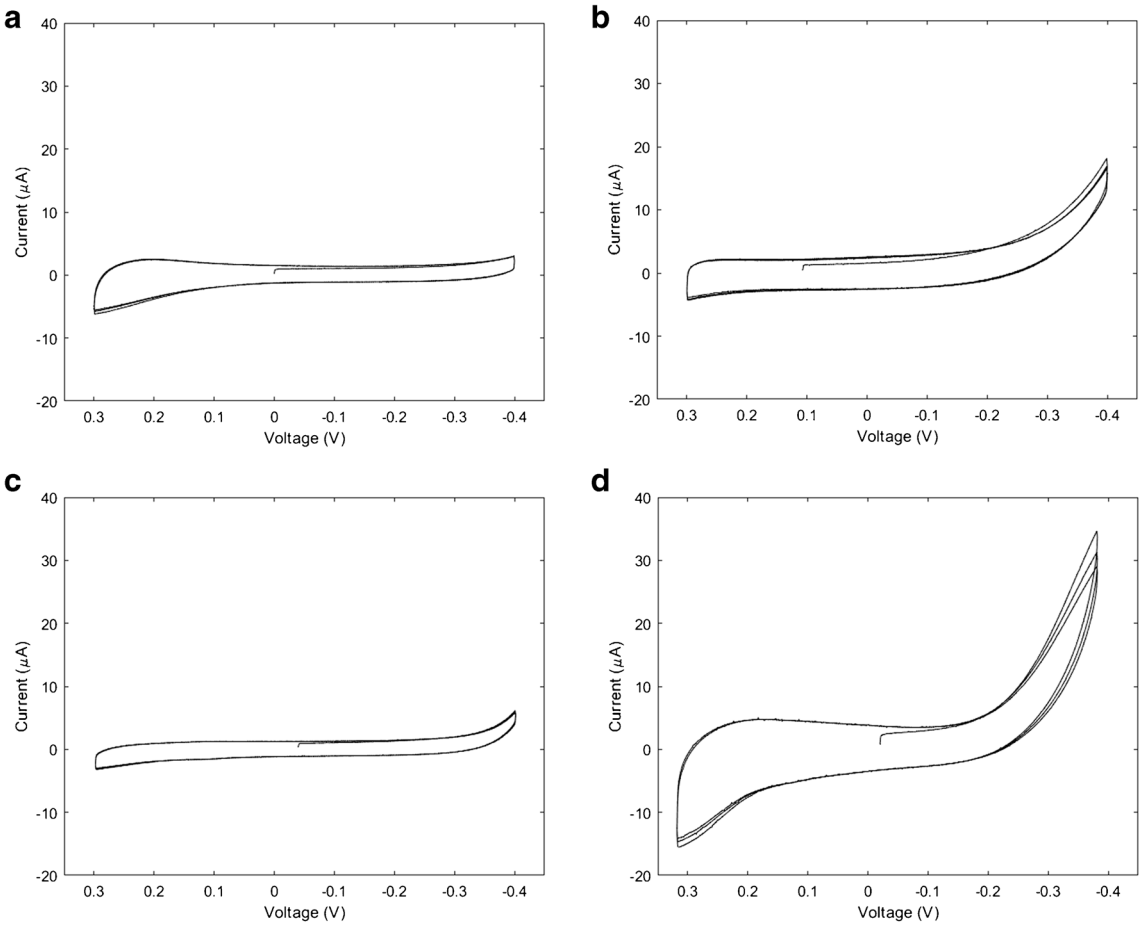

Fig. 3 Cyclic voltammograms from +300 mV to −400 mV with reference to an Ag/AgCl reference electrode for a TEGT monolayer (**a**), a Biotin–KKKKC monolayer (**b**), a 1:16 Biotin–KKKKC/TEGT monolayer (**c**), and a bare Au sensor (**d**). All cyclic voltammograms were performed in 100 mM PBS (pH = 7, 20 °C)

observed dissipation values of each surface after exposure to neutravidin remained in the acceptable range for the use of the Sauerbrey relationship (Eq. 1) to quantify the adsorbed mass [22].

To demonstrate our ability to minimize interference due to non-selective adsorption of neutravidin onto SAM-coated surfaces, we performed control experiments on TEGT-coated surfaces and bare gold surfaces. These control experiments demonstrate that bare gold exhibits substantial nonspecific adsorption of neutravidin (Fig. 4D). As expected, there was very little (<15 ng cm^{-2}) unselective neutravidin adsorption on TEGT-coated surfaces compared to ~500 ng cm^{-2} due to unselective adsorption on the bare gold surface. Monolayers prepared from 100% Biotin-KKKC on the other hand impart neutravidin selectivity adsorbing >600 ng cm^{-2} (Fig. 4C). This selectivity cannot be well-controlled by changing the

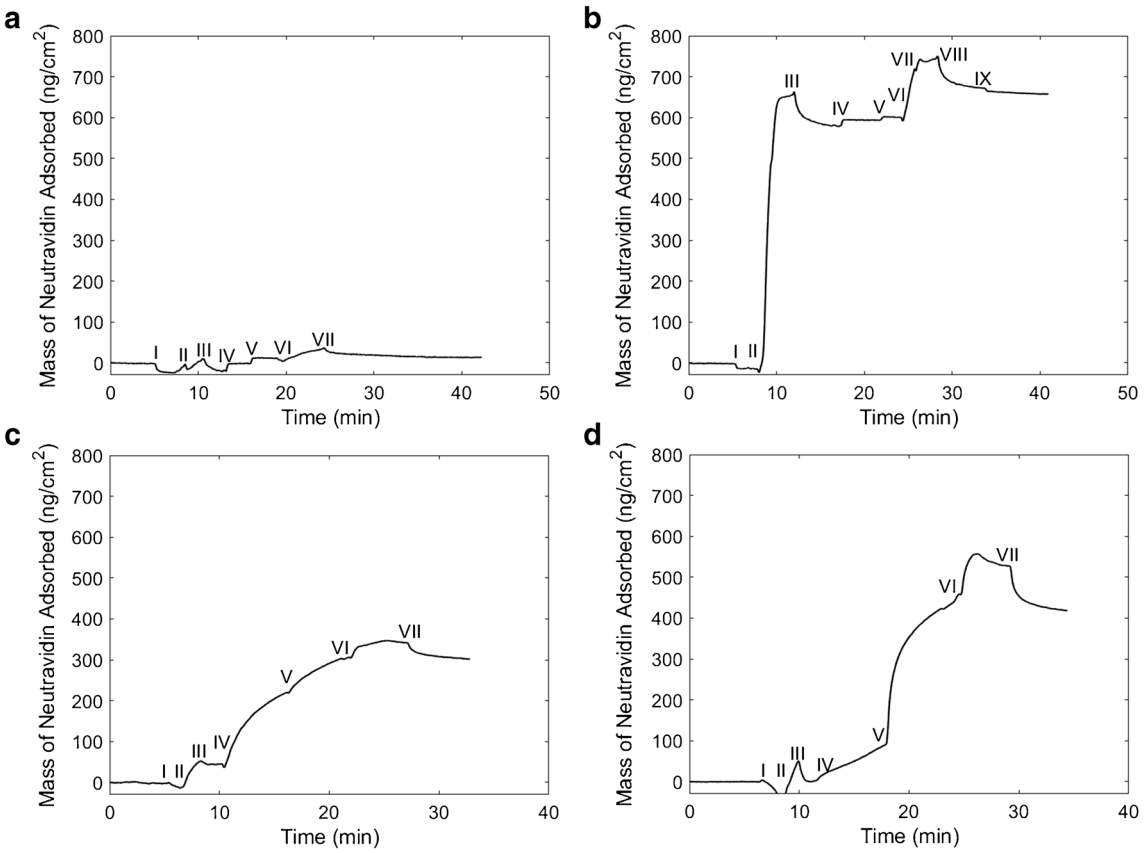

Fig. 4 Representative measurement of the mass of adsorbed neutravidin mass to a TEGT SAM (**a**), Biotin–KKKKC SAM (**b**), mixed Biotin–KKKKC/TEGT monolayer (**c**), and a bare gold surface (**d**) calculated using Eq. 1 and QCM frequency measurements (normalized to the third overtone, i.e., $\Delta f = \Delta f_3/3$). The baseline was established at OCP (+155 ± 59 mV) n 100 mM PBS solution with the pump turned off. The numerals indicate the application of −400 mV to the surface (I), the introduction of neutravidin solution at 200 µL min^{-1} (II), the reduction of pump speed to 10 µL min^{-1} (III), the surface returning to OCP (IV), the application of +300 mV to the surface (V), the surface returning to OCP and the start of a 5-min PBS rinse at 200 µL min^{-1} (VI), and the deactivation of the pump (VII). Due to the large amount of neutravidin bound by a Biotin–KKKKC SAM, the procedure for B was as follows: application of −400 mV to surface (I), introduction of neutravidin at 200 µL min^{-1} (II), 2-min rinse with 100 mM PBS at 200 µL min^{-1} (III), pump off (IV), the surface returning to OCP (V), the application of +300 mV to the surface (VI), reintroduction of neutravidin solution for 1 min at 200 µL min^{-1} (VII), 2-min rinse with 100 mM PBS at 200 µL min^{-1} (VIII), and deactivation of the pump (IX)

electrode potential, but nevertheless demonstrates neutravidin selectivity. Thus, unselective adsorption onto gold surfaces can be prevented by TEGT monolayers, and Biotin–KKKKC monolayers impart neutravidin selectivity.

For each of our replicate measurements for the mixed monolayer composed of Biotin–KKKKC and TEGT (1:16 ratio), statistically insignificant neutravidin binding of 14 ± 22 ng cm^{-2} occurred at −400 mV (Fig. 5C, Table 2). When we released the applied potential and allowed the surface to return to OCP, we observed an increase in neutravidin binding consistent with a change in conformation described previously [13, 16, 17] (Fig. 4C). The observed increase in neutravidin binding at OCP was highly variable between trials but was intermediate to the adsorption at −400 mV and +300 mV for each run. The variability likely arose from variation in the molecular density and biotin content of the mixed monolayers between experiments. At +300 mV, the biotin head groups were exposed to neutravidin, resulting in the maximum amount of binding of 210 ± 110 ng cm^{-2} (Fig. 4C, Table 2).

As described above, we repeated the same procedure with TEGT, Biotin–KKKKC, and bare gold to compare the tunability of the neutravidin binding behavior of each surface. The TEGT surface adsorbed 0 ± 5.3 ng cm^{-2} (error of single measurement)[1] at −400 mV and adsorbed 14.9 ± 5.3 ng cm^{-2} (error of single measurement) at +300 mV

[1] Error of QCM single measurement found using the upper limit of normalized standard error in QCM measurements of 0.3 Hz. The error was multiplied by the mass sensitivity constant of −17.7 ng Hz^{-1} cm^{-2} to calculate the error of a single measurement for adsorbed mass.

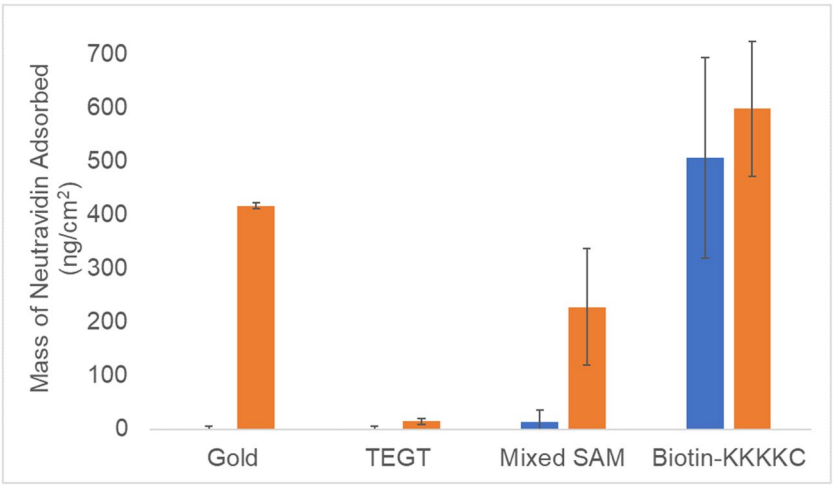

Fig. 5 Neutravidin adsorption behavior of gold, TEGT, the mixed monolayer, and Biotin–KKKKC at −400 mV (blue) and +300 mV (orange). The error bars indicate the 95% confidence interval for the Biotin–KKKKC and mixed SAMs and the error of a single measurement for the TEGT SAM and the bare Au surface

Table 2 Full range of neutravidin adsorption of TEGT, Biotin–KKKKC, Biotin–KKKKC/TEGT, and bare Au surfaces from −400 mV to +300 mV

Applied potential[a]	Average mass of adsorbed neutravidin (ng cm^{-2})[b]			
	TEGT[d]	Biotin–KKKKC[e]	Mixed SAM[e]	Au[d]
−400 mV[c]	0.0 ± 5.3	510 ± 190	~14 ± 22	0.0 ± 5.3
+300 mV	14.9 ± 5.3	600 ± 130	210 ± 110	417.2 ± 5.3

[a]With reference to Ag/AgCl electrode

[b]Mass calculated using Eq. 1 and QCM frequency measurements (normalized to the third overtone, i.e., $\Delta f = \Delta f_3/3$)

[c]Upper limit of adsorption at −400 mV prior to buffer rinse

[d]For TEGT and Au, the uncertainty corresponds to the normalized standard error of a single measurement from the QCM

[d]Uncertainty for the Biotin–KKKKC and mixed SAM corresponds to the 95% confidence interval

(Table 2). The TEGT significantly passivated the surface compared to the other surfaces used in the experiment. The Biotin–KKKKC SAM adsorbed 510 ± 190 ng cm^{-2} (95% CI) at −400 mV and 600 ± 130 ng cm^{-2} (95% CI) at +300 mV.

The Biotin–KKKKC surface did not demonstrate significantly different neutravidin adsorption behavior in response to changes in applied potential. Since the entire surface is covered with Biotin–KKKKC molecules, each Biotin–KKKKC would be sterically hindered from undergoing the conformation change when −400 mV is applied to the surface. As a result, the biotin head group remains available to bind neutravidin in the Biotin–KKKKC SAM even during the application of −400 mV.

While investigating the full range of neutravidin binding, we noted that neutravidin was able to bind nonspecifically to bare gold over time (Fig. 4D). At −400 mV, 0.0 ± 5.3 ng cm^{-2} (error of single measurement) of neutravidin was adsorbed and 417.2 ± 5.3 ng cm^{-2} (error of single measurement) was adsorbed at +300 mV. The isoelectric point of neutravidin is ~pH = 6.3 so at the experimental conditions of pH = 7, neutravidin has a slight negative charge [24]. As a result, applying −400 mV repelled the neutravidin from the gold surface and prevented the nonspecific binding of neutravidin. When the surface returned to OCP and was no longer negatively charged, neutravidin began to gradually bind to the gold surface due to electrostatic attraction (Fig. 4D, IV–V). Upon application of +300 mV, the negatively charged neutravidin would interact more favorably with the gold surface, leading to substantial nonspecific neutravidin binding.

It is important to note that while gold has the largest change in sensitivity to neutravidin in response to an applied potential, the gold surface lacks the specificity of the biotin–neutravidin interaction and thus is not practical for biosensor design. Gold surfaces nonspecifically bind other proteins [25], DNA [26], and IgG antibodies [7, 27], reducing the efficacy of nonfunctionalized gold surfaces in biosensors. This observation highlights the need for a high surface coverage of species that prevent nonspecific adsorption, like TEGT, on Au surfaces to prevent nonspecific interactions from the analyte or matrix with exposed gold. The bound neutravidin on the gold did not seem to be reversibly adsorbed as there was little mass loss upon

returning to OCP and when the surface was rinsed with buffer solution.

Another important consideration is the timescale of analysis in these experiments. Importantly, the relatively long timescales for equilibration of the changes in frequency (on the order of 5–15 min, Fig. 4) are constrained by diffusion and the kinetics of adsorption onto the QCM sensor surface. These limitations can also be seen in the case of monolayer formation, also a diffusion/adsorption-limited process, where it takes on the order of 5–10 min for frequency changes to stabilize after the addition of the thiol molecules used to form the monolayers (Fig. 2). It is therefore not surprising that the same diffusion/adsorption processes that prolong monolayer formation also prolong equilibration in experiments measuring the neutravidin adsorption. The limitations of signal drift could be addressed by allowing the sensors more time for equilibration, which indicates an important balance between signal stability and analysis time that would need to be considered in developing quantitative assays using voltage-switchable monolayers for EQCM analysis.

Conclusions

Our results confirm the formation of self-assembled monolayers with real-time voltage-tunable affinity for avidin using Biotin–KKKKC and TEGT. Our results show that the QCM is effective in detecting real-time changes in analyte binding behavior with voltage-switchable bio-surfaces, allowing observation of the evolution of surface adsorption as the applied voltage is shifted. We demonstrated the full range of the tunability of the mixed Biotin–KKKKC/TEGT surface's sensitivity to neutravidin by taking the surface from low, intermediate, to high degrees of neutravidin binding by varying the applied potential in real time. We demonstrated that the mixed monolayer surface is the most voltage responsive in terms of neutravidin binding compared to Biotin–KKKKC and TEGT surfaces. The bare gold surface had the highest tunability of neutravidin binding in response to applied potentials. However, this tunability lacked the selectivity of the surfaces containing biotinylated molecules, underscoring the importance of passivating gold surfaces to minimize the nonspecific adsorption onto bare gold. Due to its high sensitivity to changes in adsorbed mass, EQCM is a very useful approach to real-time monitoring of protein adsorption on electroactive surfaces, allowing for kinetic studies of adsorption events. Voltage-responsive biosensors coupled with QCM allow for real-time adsorption behavior of electroactive surfaces and may be suitable for disease detection, separations, and other adsorption-dependent analytical techniques.

Acknowledgements We gratefully acknowledge the gift of Biotin–KKKKC from Paula Mendes (University of Birmingham).

Author contribution NEP conducted the experiments and wrote the manuscript. WFP and PMM designed the experiments and edited the manuscript.

Funding The authors received funding from the Brigham Young University Department of Chemistry Earl M. Woolley Award.

Declarations

Conflict of interest The authors declare no competing interests.

References

1. Hayashi G, Hagihara M, Dohno C, Nakatani K. Photoregulation of a peptide−RNA interaction on a gold surface. J Am Chem Soc. 2007;129(28):8678–9. https://doi.org/10.1021/ja071298x.
2. Yousaf MN, Houseman BT, Mrksich M. Turning on cell migration with electroactive substrates We are grateful for support of this work by DARPA and the National Institute of Health (GM 54621). This work used facilities of the MRSEC supported by the National Science Foundation (DMR-9808595). M. M. is a Searle Scholar and an A. P. Sloan Fellow. B. T. Houseman is supported by MD/PhD Training Grant HD-09007. Angew Chem Int Ed Engl 2001;40(6):1093-1096. From NLM.
3. Yeo W-S, Mrksich M. Electroactive self-assembled monolayers that permit orthogonal control over the adhesion of cells to patterned substrates. Langmuir. 2006;22(25):10816–20. https://doi.org/10.1021/la061212y.
4. Yousaf MN, Houseman BT, Mrksich M. Using electroactive substrates to pattern the attachment of two different cell populations. Proc Nat Acad Sci. 2001;98(11):5992–6. https://doi.org/10.1073/pnas.101112898.
5. Chan EWL, Yousaf MN. Immobilization of ligands with precise control of density to electroactive surfaces. J Am Chem Soc. 2006;128(48):15542–6. https://doi.org/10.1021/ja065828l.
6. Verger F, Colas F, Sire O, Shen H, Rinnert E, Boukerma K, Nazabal V, Boussard-Plédel C, Bureau B, Toury T et al. Surface enhanced infrared absorption by nanoantenna on chalcogenide glass substrates. Appl Phys Lett 2015;106(7):073103. https://doi.org/10.1063/1.4913308. (acccessed 6/24/2024).
7. Liu Y, Mu L, Liu B, Zhang S, Yang P, Kong J. Controlled protein assembly on a switchable surface. Chem Commun. 2004;10:1194–5. https://doi.org/10.1039/B400776J.
8. Mendes PM. Stimuli-responsive surfaces for bio-applications. Chem Soc Rev. 2008;37(11):2512–29. https://doi.org/10.1039/b714635n.
9. Callari FL, Petralia S, Conoci S, Sortino S. Light-triggered DNA release by dynamic monolayer films. New J Chem. 2008;32(11):1899–903. https://doi.org/10.1039/b808118b.
10. Mu L, Liu Y, Cai S, Kong J. A smart surface in a microfluidic chip for controlled protein separation. Chemistry. 2007;13(18):5113–20. https://doi.org/10.1002/chem.200601624FromNLM.
11. Mendes PM, Christman KL, Parthasarathy P, Schopf E, Ouyang J, Yang Y, Preece JA, Maynard HD, Chen Y, Stoddart JF. Electrochemically controllable conjugation of proteins on surfaces. Bioconjugate Chem. 2007;18(6):1919–23. https://doi.org/10.1021/bc7002296.
12. Hook AL, Chang C-Y, Scurr DJ, Langer R, Anderson DG, Williams P, Davies MC, Alexander MR. Thermally switchable polymers achieve controlled Escherichia coli detachment. Adv Healthc

Mater. 2014;3(7):1020–5. https://doi.org/10.1002/adhm.201300518.
13. Yeung CL, Iqbal P, Allan M, Lashkor M, Preece JA, Mendes PM. Tuning specific biomolecular interactions using electro-switchable oligopeptide surfaces. Adv Funct Mater. 2010;20(16):2657–63. https://doi.org/10.1002/adfm.201000411.
14. Zhang L, Wang Z, Das J, Labib M, Ahmed S, Sargent EH, Kelley SO. Potential-responsive surfaces for manipulation of cell adhesion, release, and differentiation. Angew Chem Int Ed. 2019;58(41):14519–23. https://doi.org/10.1002/anie.201907817.
15. García-Fernández A, Lozano-Torres B, Blandez JF, Monreal-Trigo J, Soto J, Collazos-Castro JE, Alcañiz M, Marcos MD, Sancenón F, Martínez-Máñez R. Electro-responsive films containing voltage responsive gated mesoporous silica nanoparticles grafted onto PEDOT-based conducting polymer. J Contr Release. 2020;323:421–30. https://doi.org/10.1016/j.jconrel.2020.04.048.
16. Cantini E, Wang X, Koelsch P, Preece JA, Ma J, Mendes PM. Electrically responsive surfaces: experimental and theoretical investigations. Acc Chem Res. 2016;49(6):1223–31. https://doi.org/10.1021/acs.accounts.6b00132.
17. Yeung CL, Wang X, Lashkor M, Cantini E, Rawson FJ, Iqbal P, Preece JA, Ma J, Mendes PM. Modulation of biointeractions by electrically switchable oligopeptide surfaces: structural requirements and mechanism. Adv Mater Interfaces 2014;1(2):1300085. https://doi.org/10.1002/admi.201300085. (acccessed 2024/06/24).
18. Lahann J, Mitragotri S, Tran T-N, Kaido H, Sundaram J, Choi IS, Hoffer S, Somorjai GA, Langer R. A reversibly switching surface. Science 2003;299(5605):371-374. https://doi.org/10.1126/science.1078933. (acccessed 2024/06/24).
19. Lippert D, Burnham J, Seo D. Active control of contact angles of various liquids from the response of self-assembled thiol molecules to electric current. Langmuir. 2023;39(14):5021–30. https://doi.org/10.1021/acs.langmuir.3c00026.
20. Green NM. AVIDIN. 3. The nature of the biotin-binding site. Biochem J. 1963;89(3):599–609. https://doi.org/10.1042/bj0890599.
21. Sauerbrey G. Verwendung von Schwingquarzen zur Wägung dünner Schichten und zur Mikrowägung. Zeitschrift Für Physik. 1959;155(2):206–22. https://doi.org/10.1007/BF01337937.
22. Reviakine I, Johannsmann D, Richter RP. Hearing what you cannot see and visualizing what you hear: interpreting quartz crystal microbalance data from solvated interfaces. Anal Chem. 2011;83(23):8838–48. https://doi.org/10.1021/ac201778h.
23. Wang S, Huang X, Shan X, Foley KJ, Tao N. Electrochemical surface plasmon resonance: basic formalism and experimental validation. Anal Chem. 2010;82(3):935–41. https://doi.org/10.1021/ac902178f.
24. https://www.thermofisher.com/order/catalog/product/31050. Retrieved 6/24/2024.
25. Mrksich M. A surface chemistry approach to studying cell adhesion. Chem Soc Rev. 2000;29(4):267–73. https://doi.org/10.1039/a705397e.
26. Yu ZL, Yang CWT, Triffaux E, Doneux T, Turner RFB, Bizzotto D. Measuring and remediating nonspecific modifications of gold surfaces using a coupled in situ electrochemical fluorescence microscopic methodology. Anal Chem. 2017;89(1):886–94. https://doi.org/10.1021/acs.analchem.6b03953.
27. Rastogi A, Nad S, Tanaka M, Mota ND, Tague M, Baird BA, Abruña HD, Ober CK. Preventing nonspecific adsorption on polymer brush covered gold electrodes using a modified ATRP initiator. Biomacromolecules. 2009;10(10):2750–8. https://doi.org/10.1021/bm900564t.